研 究 論 文

大 韓 熔 接 學 會 誌
第5卷, 第1號, 1987年 3月
Journal of the Korean Welding Society
Vol. 5, No. 1, Mar., 1987

Arc Efficiency and Kerf Width in Plasma Arc Cutting Process

T. J. Lho*, S. J. Na**

플라즈마 절단공정에서의 아아크 효율과 절단폭

노 태 정*·나 석 주**

Keyword : Plasma Cutting(플라즈마절단), Arc Efficiency(아아크효율), Kerf Width(절단폭), Heat Flow(열유동), Heat Input Ratio(열입의 비율)

초 록

플라즈마 절단은 산업계에서 널리 사용되고 있으나 공정의 해석에 대한 연구는 매우 부족하다. 본 연구에서는 알미늄판재에 나타나는 온도분포를 해석함으로써 절달폭을 이론적으로 예측하고자 하였다. 열유동을 해석하는데 있어서, 플라즈마 아아크의 강도가 폭방향으로는 정상분포(Gaussian distribution)을 갖고 두께방향으로는 지수함수적으로 감소한다고 가정하였다. 측정된 아아크효율을 이용한 계산결과 이론적으로 예측된 절단부의 크기 및 형상이 실험치와 매우 잘 일치하였으며, 따라서 제안된 해석방법은 플라즈마 절달공정의 해석에 유용하게 적용될 수 있었다.

Abstract

Plasma arc cutting is a fusion cutting process in which a gas constricted arc is employed to produce high temperature, high velocity jet at the workpiece. Even though the plasma arc cutting has been widely used in the industry, very little work has been done on the analysis of the process. In this paper, the kerf width was numerically analyzed by soving the temperature distribution in base metal under consideration of the latent heat effect. In modelling the heat flow problem, the heat intensity of the plasma arc was assumed to have a Gaussion distribution in the transverse direction and exponentially decreasing in the thickness direction. The thermal efficiency and the heat input ratio of the top surface were experimentally deterimned for various thickness and cutting conditions, and used in numerical calculation of the kerf width. The experimental results were in considerabely good agreement with the theoretically predicted kerf width.

* Samsung Shipbuilding & Heavy Industries Co., Ltd.
** Membr, Department of Production Engineering, Korea Advanced Institute of Science and Technology

1. Introduction

Plasma arc cutting, which was discovered in the early 1950's, is a thermal process wich severs metals by melting a localized area with the heat of a constricted arc and by removing the molten material with a high velocity jet of hot, ionized gas issuing from the orifice. The principle of the operation is as follows: The pilot arc, which is the spark between the electrode and nozzle, significantly heats the orifice gas, thereby greatly increases its ionization. The ionized gas then passes through the nozzle, and if is close enough to the workpiece, it creates a path for the main cutting arc to strike. [1]

The plasma arc cutting process provides some distinct advantages such as increased travel speed, excellent working accuracy and cutting of the special materials (those are Al-alloys and stainless steels etc.) compared to the conventional thermal cutting processes such as oxy-acetlene cutting and air carbon arc cutting. Several investigators have long reported their findings in studies of the plasma arc cutting process. [2]-[6] However, most of them have analyzed the plasma arc cutting process only qualitatively, and very little work has been done on the quantitative analysis of the kerf width, even if the effectiveness and quality of the plasma arc cutting are closely linked with the kerf width of the resulting cut. In this paper, the kerf width was analyzed mathematically by solving the heat flow problem in base metal with the assumed heat intensity distribution of the plasma arc. And a series of experiments was carried out with an Al-alloy to determine the thermal efficiency and to confirm the accuracy of the theoretical analysis.

2. Theoretical formulation

The heat requried for kerf formation in the plasma arc cutting is supplied by the high temperature, high heat intensity plasma arc and by electrons in anode spots. This heat elevates the workpiece locally up to the melting temperature, and if the additional latent heat is supplied, this heated area will undergo the phase change into the liquid state, Since this process is, in the strict sense of the word, a non-stationary process, the theoretical analysis of the plasma arc cutting process is quite complex. If a very long cutting is being made, however, non-stationary effects are important only at beginning and ending of the process. During most of the cutting process, the temperature distribution observed in a coordinate system moving with the arc will appar to b e stationary, as shown in Fig. 1. To analyze the kerf width, the energy equilibrium and the temperature distribution in the base metal are to be investigated for the quasi-stationary state.

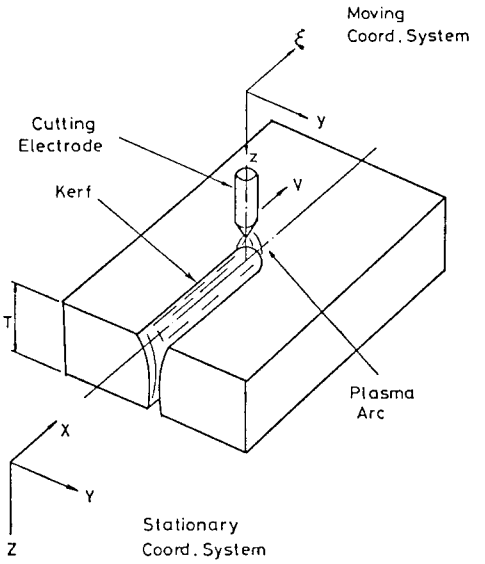

Fig. 1. Coordinate systems for the analysis of plasma arc cutting process

2-1. Electron effects at the anode

The anode spots are the portion of the base metal in which the electrons of the arc are absorbed. Through the super high-speed filming of the cutting process, [2] it was found that anode spots move rapidly to the lower part of the cut at about several kHz, since the workpiece is removed progress-

ively. The heat supplied to the base metal by the anode spots equals to : [7]

$$Q_a=(\Phi_e+TE+V_a)\,I \qquad (1)$$

where Q_a is the heat supplied to the base metal by the anode spots, V_a is the anode voltage drop, TE is the electron thermal energy, Φ_e is the work function of the base metal, and I is the arc current. As presented in Ref. 8, the characteristic values for the used Al-alloy were chosen as folows: $\Phi_e=4$ volts, $TE=1$ volt, and $V_a=1$ volt. In several papers, it was reported that the anode spots occur only in the limited area of the cutting edge.[2],[4] In this study, however, it was assumed that the frequency of the anode spot generation is uniform through the cut edge of the base metal to simplify the modelling of the cutting pheomena.

2-2. Shape and heat intensity of the plasma arc

In general, the photographic and rotating probe method have been used to anlyze the of plama arc,[9],[10] which is influenced mainly by the gas pressure, the nozzle shape and the arc current. In this study, the shape of the plasma arc was determined by the following equation proposed by E.M. Esiban & M.E. Danchenko.[2]

$$W_a=D_n+\chi h \qquad (2)$$

Where W_a is the diameter of plasma arc at the top surface of the base metal in cm, D_n is the nozzle diameter in cm, χ is a correction coefficient and h is the arc length in cm, as illustrated in Fig. 2. Assuming that χ is closed to 0.1, and substituting $D_n=1.5$mm and $h=4$mm into eq. (2), the value of W_a becomes 1.9mm. This calculated value was in satisfactorily good agreement with the actual shape of the plasma arc determined by the photographic method. Subtracting the conduction loss at tho nozzle and the radiation loss to the atmosphere from the total plasma arc energy, the plasma arc power Q_p(in J/sec) canbe expressed by

$$Q_p=\eta_p V_p I \qquad (3)$$

where η_p is the plasma efficiency and V_p is the plasma arc voltage drop in volts. It was reported that the energy losses at the cathode, at the nozzle and in the atmosphere are 3%, 10%, and 10% of the total power, respectively.[3] η_p becomes then to be 77%, which was accepted also in this study. The heat intensity distribution of the plasma arc was calculated quantitieely by using the U.V.O. (Ultra-violet oscilloscope) traces.[9] Other investigators also analyzed the heat intensity distribution hydrodynamically by assuming that the plasma jet is a turbulent flow.[2] All the results showed that the heat intensity distribution of the plasma arc can be fairly well represented by a Gaussian form.[8],[10]-[12]

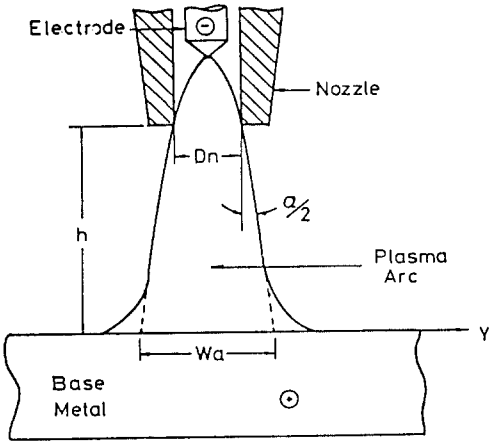

Fig. 2. Shape of the plasma arc

2-3. Heat epuilibrium in the plasma arc cutting process

The heat required for kerf formation is supplied to the base metal by the plama arc and by the anode spots. And a portion of this heat is released in the form of ejected plasma without effecting the base metal. The equations for the heat equilibrium are, therefore, expressed as follows :

$$V_p=V_t-(\Phi_e+TE+V_a) \qquad (4)$$

$$Q_p+Q_a=Q_{av}+Q_{ep} \qquad (5)$$

$$Q_{av}=\eta_a Q_p+(\Phi_e+TE+V_a)I \qquad (6)$$

$$Q_{av}=Q_c+Q_l \qquad (7)$$

where, V_t : total arc voltage drop [volts]

Q_{av} : available heat input rate for forming the kerf [J/sec]

Q_{ep} : power of the ejected plasma [J/sec]

η_a : arc efficiency

Q_c : heat input rate for conduction in the base metal [J/sec]

Q_l : latent heat rate of the molten base metal [J/sec]

The arc efficiency η_a is a process constant defined as the ratio of the heat available for the cutting itself to the heat transferred to the workpiece by plasma arc voltage drop, and was determined experimentally by using a calorimeter. From equation(6) the arc efficiency is defined as follows :

$$\eta_a = (Q_{av} - (\Phi_e + TE + V_a)I)/Q_p \tag{8}$$

2-4. Heat intensity and temperature distribution

The governing equation of the quasi-stationary heat flow in the base metal due to the line heat source having a constant intensity and moving at a constant speed can be expressed by the following equation, Fig. 1.

$$\frac{\partial^2\theta}{\partial\xi^2} + \frac{\partial^2\theta}{\partial y^2} = -\frac{v}{\lambda}\left(\frac{\partial\theta}{\partial\xi}\right) \tag{9}$$

The initial condition is

$$\theta|_{t=0} = \theta_0 \tag{10}$$

and the boundary conditions are as follows :

$$-2\pi r\, Tk\left(\frac{\partial\theta}{\partial r}\right) \to Q_c \quad as \quad r \to 0 \tag{11}$$

$$\theta = \theta_0 \text{ as } r \to \infty \tag{12}$$

where, ξ, y, z : moving coordinate system

t : time [sec]

θ : temperature at time t [°C]

θ_0 : initial temperature [°C]

Q_c : heat input rate [J/sec]

T : thickness of the base metal [cm]

k : thermal conductivity [J/g°C sec]

λ : thermal diffusivity [cm²/sec]

p : density of the material [g/cm³]

c : specific heat [J/g°C]

v : cutting speed [cm/sec]

r : distance from the line heat source[cm]

$= \sqrt{\xi^2 + y^2}$

Assuming that the thermal properties of the base metal do not change with temperature and the convective and radiative heat loss from the workpiece surface is negligible, the temperature distribution in the base metal can be expressed as follows :

$$\theta - \theta_0 = \frac{q_c}{2\pi k} e^{-(v/2\lambda)\xi}\, K_0\left(\frac{vr}{2\lambda}\right) \tag{13}$$

where K_0 is the zero order modified Bessel function of the second kind and q_c is the heat input rate per unit length of the line heat source ($q_c = Q_c/T$). In this study, the considered distance from the heat source r was relatively small since temperature distribution was calculated mainly for the molten zone near the heat source. The Bessel function K_0 should be, therefore, evaluated by using a series representation.[15],[16]

Assuming that the heat intensity of the plasma arc decreases exponentially in the thickness direction, the heat input rate per unit length can be expressed under the consideration of uniform anode spots by the following equations, Fig. 3.

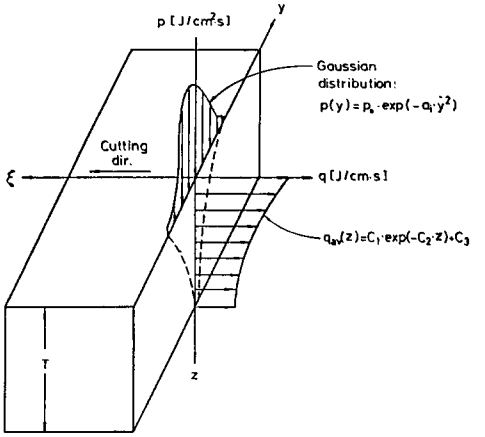

Fig. 3. Assumed heat intensity distribution of the plasma arc

$$q_{av}(z) = C_1 e^{-C_2 z} + C_3 \tag{14}$$

$$\int_0^T q_{av}(z)dz = Q_{av} \tag{15}$$

$$C_3 = (\Phi_e + TE + V_a)I/T \tag{16}$$

q_{av} on the top surface can be given by

$$q_{av}(z)\Big|_{z=0} = \mu(Q_{av}/T) \tag{17}$$

where, $q_{av}(z)$: heat input rate per unit length in the thickness direction [J/sec cm]

C_1, C_2, C_3 : constants

μ : heat input ratio of the workpiece top surface to the average heat input

The variation of the heat input rate per unit length in the thickness direction can be then obtained by combining the equations (4), (6) and (14)-(17).

In the transverse direction, the variaton of the plasma arc intensity was assumed to have a rectangular Gaussian distribution. Assuming that the maximum heat input rate per unit area at center ($y=0$) is p_0, the heat input rate in the y-axis can be expressed as follows :

$$p(y)=p_0e^{-ay^2} \tag{18}$$

With these assumptions on the heat input rate in the thickness and transverse direction, the analytic determination of the equation (13) is generally impossible or quite difficult, if possible. The total thickness of the workpiece was, therefore, divided into a appropriate number of stocks and the temperature distribution was determined numerically in each stock to analyze the variation of the kerf width in the thickness direction.

The heat input rate per unit length in the i-th stock $q_{av}[i]$ can be expressed by

$$q_{av}[i]=\int_{-\bar{y}_i}^{\bar{y}_i} p_0e^{-a_iy^2}\,dy \tag{19}$$

wher $\bar{y}_i$ and a_i are Gaussian constants for the *i-th* stock. Assuming that the heat input rate at $y=\bar{y}_i$ corresponds to 5% of the maximum value(p_0), the following relationship is obtained from equation(18).

$$0.05\ p_0=p_0e^{-a_i\bar{y}_i^2} \tag{20}$$

Assuming that the maximum heat input rate per unit area p_0, which is determined for first stock using the empirically determined value of μ, is same in each stock, the variation of the heat intensity in the thickness and transverse direction can be determined by obtaining the characteristic values of the Gaussian distribution p_0, $\bar{y}_i$, a_i from the equations (19) and (20).

Each stock was divided again into a number of elements in the transverse direction to determine the temperature distribution numerically, Fig. 4. The heat inpt rate on the element located at $y=y^*$ can be then expressed by

$$q_{ic}=p_0e^{-a_iy^{*2}}\ (2\bar{y}_i/(Ne-1)) \tag{21}$$

where q_{ic} is the intensity of the line heat source located at $y=y^*$ of the *i-th* stock and Ne is the number of transverse elements. The temperature

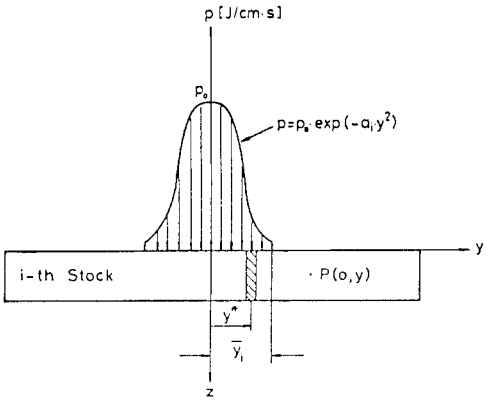

Fig. 4. Assumed transverse heat intensity distribution in the i-th stock

rise at a point $P(0, y)$ by a line heat source at $y=y^*$ is obtained from the equations (13) and (21). The total temperature rise at the point $p(0, y)$ can be then determined by superoposing the effects of each heat source as follows.

$$\theta-\theta_0=\int_{-\bar{y}_i}^{\bar{y}_i}\frac{p_0}{2\pi k}e^{-a_iy^{*2}}e^{-(v/2\lambda)\xi}K_0\left(\frac{vr}{2\lambda}\right)dy^*. \tag{22}$$

The integration of the above equation was carried out numerically by using the Simpson's rule.

In a quasi-stationary heat flow problem such as in the welding process, the temperature distribution in the base metal is continuously influenced by the moving heat source, even after the heat source has passed the reference x-position (i.e., $\xi<0$). In this study, however, the effect of the heat source was neglected for the ξ-value less than zero, because in the cutting process the molten metal near the heat source is promptly removd by the cutting gas. Therefore, it can be assumed that the maximum temperature at the point (ξ, y) in the transverse direction is obtained just as the heat source passes the reference point (*i.e.*, $\xi=0$).

The latent hast is defined as the heat required for the phase change from solid to liquid at the melting temperature or interval. In case of pure metals, the phase changes at a constant temperature, while the phase change of metal alloys occurs gradually with the increasing temperature from solidus to liquidus temperature. Assuming that the

portion of the liquid phase increases linearly with the increasing temperature, the temperature distribution was determined by using the iterative method as follows :

(1) Assume the initial portion of the conduction heat

(2) Calculate the temperature distribution by using the equation (22)

(3) Determine the latent heat required for the fully and partially molten zone.

(4) Compare the results of the step 3 with the assumed portion of the latent heat.

i) If the difference is within the error bound, stop the iteration

ii) If the difference is larger than the error limit, assume the new portion of the conduction heat and repeat from the step 2

3. Apparatus and procedure in the experiment

3-1. Measurement of the arc efficiency

The objective of this experiment was to investigate the variation of the are efficiency for different base metal thickness and cutting parameters. The arc efficiency was measured using a calorimeter, the schematic diagram of which is shown in Fig. 5. A agitator was used to maintain the uniform temperature in water and bronze vessel. When selecting the experimental cutting conditions, Recommendations of the machine manufacturer was considered in the first place to ensure the through-cutting, table 1. The experimental procedure was as follows:

1) Cut the specimen with the selected cutting condition

2) Put the cut specimen into the calorimeter as soon as possible to prevent the possible heat dissipation in the atmosphere

3) Agitate the water and measure the equilibrium water temperature

4) Calcuate the heat transferred to the base metal as follows :

$$Q_t = M_{se}C_s\triangle T_s + \triangle M_s(Q_{lt} + C_s\triangle T_m) + M_bC_b\triangle T_b + M_wC_w\triangle T_w \quad (23)$$

$$Q_{av} = Q_t/t_c \quad (24)$$

where, Q_t : heat transferred to the workpiece [J]

M_{si}, M_{se} : specimen mass before and after cutting, respectively [g]

$\triangle M_s$: $M_{si} - M_{se}$ [g]

M_w, M_b : mass of water and bronze vessel, respecively [g]

C_s, C_w, C_b : specific heat of specimen, water, and bronze vessel, respectively [J/g°C]

$\triangle T_s$, $\triangle T_w$, $\triangle T_b$: temperature change [°C]

$\triangle T_m$: temperature difference between initial and melting temperature of the specimen [°C]

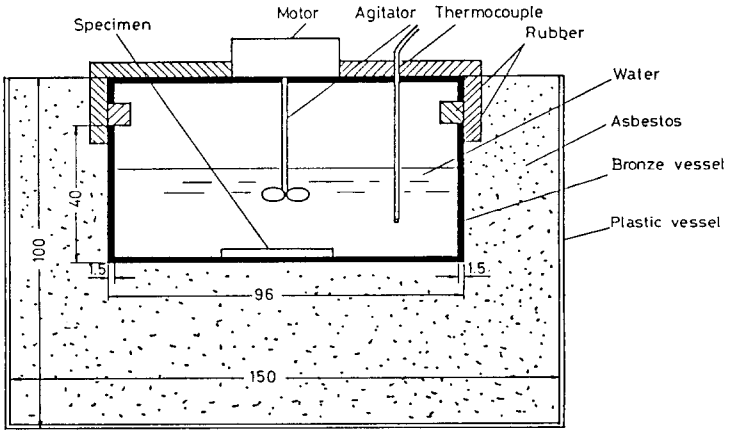

Fig. 5. Schmatic diagram of the calorimeter

Table 1. Cutting cenditions for the arc efficiency measurement

Case No	thickness (*mm*)	arc current (*A*)	arc voltage (*V*)	cutting velocity (*cm/min*)
1	4	85	100	110
2	4	85	100	90
3	4	85	100	70
4	10	95	100	40
5	10	95	100	45
6	10	95	100	50
7	16	100	110	35
8	16	100	110	40
9	16	100	110	45
10	20	100	120	30
11	20	100	120	35
12	20	100	120	40

* Shielding gas: Air $5kg/cm^2$
* Cutting gas: Ar(80%)+H_2(20%) 15 *l/min.*

Q_{lt} : latent heat of the specimen[J/g]
t_c : cutting time[sec]

The thermal properties of the experimental material Al-5052 were assumed to be constant in the calculation, table 2. With the value of Q_{av} determined experimentally from the equation (24), the arc efficiency can be calculated from the equation (8). If the effects of anode spots are neglected, a more simple form of arc efficiency η' is expressed in the following manner.

$$\eta'_a = Q_{av}/Q_p \qquad (25)$$

Table 2. Physical properties of Al 5052

Thermal diffusivity	0.5353 cm^2/s
Thermal conductivity	1.3816 $J/g.°C.s$
Latent heat	405 J/g
Specific weight	2.68 g/cm^3
Solidus temperature	593 $°C$
Liquidus temperature	649 $°C$
Work function	4 *volts*

3-2. Measurement of the heat input ratio of the top surface

To obotain the complete expression of the heat input rate along the thickness, the heat transfer rate into one stock is to be known at least, since the heat input rate per unit length was assumed to decrease exponentially in the thickness diredtion. The objective of this experiment was, therefore, to determine the ratio of the heat transfer rate into the workpiece top surface to the average value along the total thickness.

The specimen was composed of several thin aluminum sheets of 1.27mm thickness. After cutting the specimen with the cutting condition as shown in table 3, all the aluminum sheets were put into the calorimeter as a first step to determine the average value of heat input rate per unit thickness. In the next place, only the top sheet was put into the calorimeter to obtain the heat transfer rate into the top sheet. The heat input ratio of the workpiece top surface was then calculated by the follwoing eruation.

$$\mu = \frac{Q_T/M_T}{Q_t/M_t} \qquad (26)$$

Table 3. Cutting conditions for the μ-value measurement

Case No	Thickness (*mm*)	Current (*A*)	Voltage (*V*)	Velocity (*cm/min.*)	Arc eff. (η'_a)	Heat input per unit length (*J/cm*)
1	5.08	90	100	90	0.2523	1166
2	5.08	90	100	70	0.2523	1499
3	10.16	95	100	60	0.2939	2150
4	10.16	95	100	50	0.2939	2580
5	12.70	100	105	50	0.3147	3053
6	12.70	100	105	45	0.3147	3393
7	12.70	100	105	40	0.3147	3817
8	15.24	100	110	40	0.3356	4264
9	15.24	100	110	35	0.3356	4873
10	20.32	100	120	35	0.3772	5975

* Shieding gas: Air $5\,kg/cm^2$
* Cutting gas: Ar(80%)+H^2(20%) 15 *l/min.*

where, Q_T, Q_t : heat transferred into the top sheet and into the total sheets, respectively [J]

M_T, M_t : mass of the top sheet and the total sheets, respectively[g]

3-3. Measurement of the kerf width

The objective of this experiment was to investigate the kerf width variation with cutting condions and specimen thickness, The spedimens, which were used to determine the arc efficiency, were polished and photorgraphed to measure the kerf width variations in the thickness direction.

4. Results and discussions

Fig. 6 shows the variation of the measured arc efficiency versus plate thickness. The experimental results show that the arc efficiency increases almost linearly with the increasing workpiece thickness. This may be due to the fact that the penetration time of the plasma arc in cutting of the thicker plate is longer than in case of thinner plate. The solid and dotted line are calculated results by the 1st square fitting method for the case of uniform anode spots and no anode spots, respectively. It is shown that the arc efficiency can be closely related to the plate thickness by the following equations.

$\eta_a = 0.0091T + 0.1502$: uniform anode spots

$\eta'_a = 0.0082T + 0.2106$: no anode spots

The measured plasma arc cutting efficiencies are lower than the reported plasma arc welding efficiency of 60-66%[8], in fact much lower, when considering that the plasma cutting arc efficiency was defined not in comparison with the total plasma heat as in plasma welding, but in comparison with the net plasma heat in which the heat loss between the cathode and the workpiece top surface is excluded, in this study 77% of the total plasma heat. The plasma arc cutting efficiency may be expressed in the following equation, when it is defined with respect to the total plasma heat.

$$\eta''_a = 0.77 \times \eta'_a$$
$$= 0.0063T + 0.1622$$

This relationship will give the arc efficiency of 0.187 for $T = 4$mm and 0.288 for $T = 20$ mm. The low arc efficiency is mainly due to the ejected plasma in plasma arc cutting, while in plasma arc welding no plasma or only a little plasma will be ejected from the base metal.

The variation of the heat input ratio of the top surface is thown in Fig. 7 in contrast to the avail-

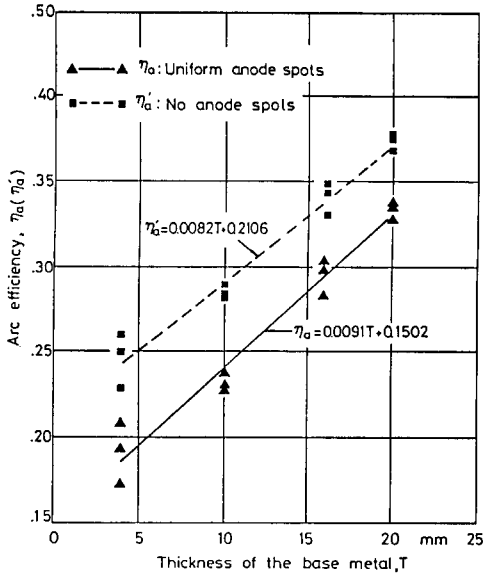

Fig. 6. Plasma cutting arc efficiency versus workpiece thickness

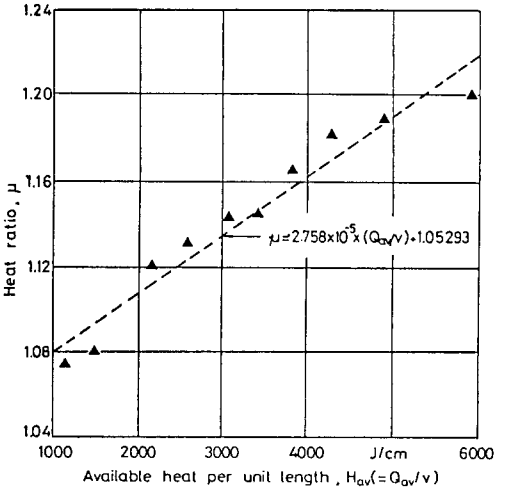

Fig. 7. Heat input ratin of the top surface versus available heat input unit length

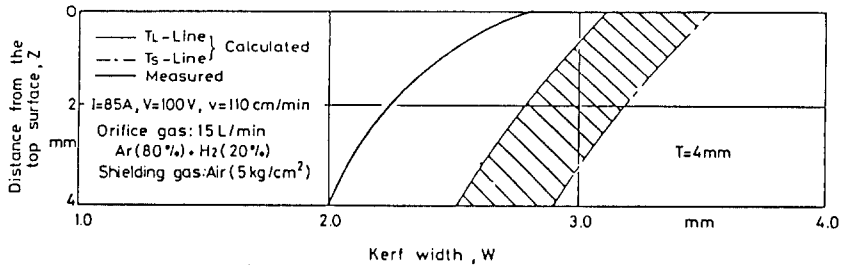

Fig. 8. Variation of the kerf width along the workpiece thickness

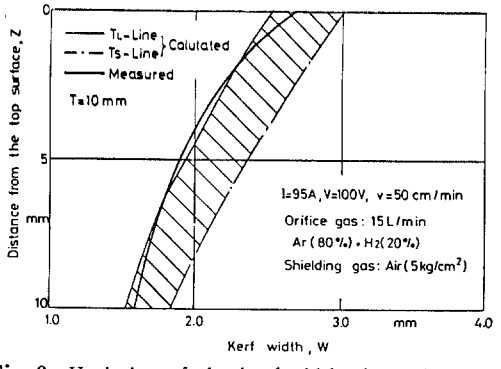

Fig. 9. Variation of the kerf width along the work piece thickness

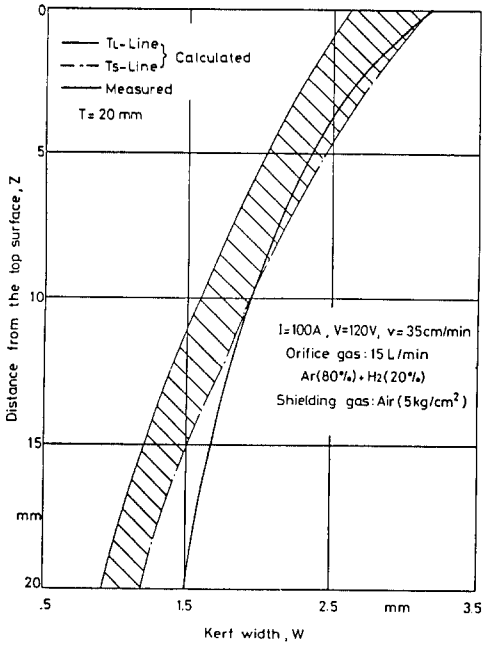

Fig. 10. Variation of the kerf width along the workpiece thickness

able heat input per unit length. It can be seen that the heat ratio increases almost linearly with the increasing available heat input per unit length, that is, more portion of the heat will be transferred to the top surface as more heat is transferred to the workpiece. The following relationship of the heat input ratio versus abailable heat per unit length was obtained by the 1st square fitting method.

$$\mu = 2.758 \times 10^{-5} \times (Q_{av}/v) + 1.05293$$

This μ -value was needed in determining the initial distribution of heal intensity in the thickness direction.

The measued and calculated kerf width variations in the thickness direction are shown in Fig. 8, 9 and 10 for various plate thickness and cutting conditions. In case of 4 mm thickness, the experimental kerf widths are considerably smaller than the calculated width of liquid zone, Fig. 8. In case of 10 mm thickness, however, the experimental kerf width coincide very closely with the calculated liquidus temperature trace, while for 20 mm thickness the experimental results are in better agreement with the calculated solidus temperature trace. This may be mainly due to the effect of gas jet pressure on removing the molten base metal and also due to the assumption adopted in solving the heat transfer equation. During Cutting of 4 mm thickness aluminum alloy, the cutting gas can pass the workpiece rather freely without removing all the molten metal, while in case of 20 mm thickness the resistance of the base metal against gas flow is high enough that also the partially molte metal will be extracted with the cutting gas. However, the calculated kerf width variations in the thickness direction show a very similar tendency as the measreud. This proves that the assumption of the exponenti-

ally decreasing heat input rate per unit length in the chickness direction is fairly reasonable. The comparison of the experimental results indicates that the kerf width at the top surface increases with the increasing plate thickness, while the kerf width at the bottom surface gradually decreases. The numerical analysis showed that the occurance of uniform anode spots has only a negligable influence on the shape and size of the kerf width, so that the calculated values obtained under consideration of no anode spots were disregarded.

5. Conclusion

A mathematical model for the determination of the kerf width in plasma arc cutting was proposed by considering the heat input rate and temperature variation in the workpiece. A series of experiments was conducted with Al-5052 for various plate thickness and cutting parameters to varify the accuracy of the proposed model and to determine the arc efficiency in plasma arc cutting process. The results of this study can be summarized as follows.

1) The plasma arc cutting efficiency increases almost linearly with the increasing workpiece thickness.
2) The plasma arc cutting efficiency is much lower than the plasma arc welding efficiency.
3) The heat input ratio of the top surface increases linearly with the increasing available heat input per unit length
4) The heat input rate from the plasma arc can be assumed to have a Gaussian distribusion in the transverse direction and an exponentially decreasing distribution in the tickness direction.
5) The proposed mathematical model can be used to determine the optimum cutting conditions for a given material and thickness and to compensate the kerf width in automatic plasma cutting.

Further research on the effect of cutting gas and other numerical approaches, such as Finite Difference Method and Finite Element Method etc., could be carried out to improve the theoretical results.

Acknowledgements

The authors gratefully acknowledge the support from the Ministry of Science and Technology, Republic of Korea.

References

1. American welding Society, *Recomended practices for plasma arc cutting*, 1982, pp. 1-5
2. K.V. Vasillev & N.I. Nikiforov, "On the factor determining the width of plasma arc cut", Svar. Proiz., No. 6, pp. 40-41
3. 松山欽一, "高速 切斷法とその 實用化", 溶接學會誌, 第43巻(1974, 8), pp. 805—817
4. 西口公之, "プラスマアーク切斷現象に關する 基礎的 研究(第1報)", 溶接學會誌, 第41巻 (1972, 7), pp. 781—791
5. 西口公之, "プラスマアーク 切斷現象に關する基礎的 研究(第2報)", 溶接學會誌, 第46巻(1977, 8), pp. 585-591
6. 西口公之, "プラスマアーク切斷現象に關する 基礎的 研究(第3報)", 溶接學會誌, 第46巻(1977, 9), pp. 616-622
7. J.F. Lancaster, *Metallurgy of welding*, George Allen & Unwin, 1980, pp. 31-39
8. J.C. Metcalfe & M.B.C. Quigley, "Heat transfer in plasma welding", W. J., Mar. 1975, pp. 99s-103s
9. C.J. Allum & B.E. Pinfold, "Some effect of shielding gas flow on argon-tungsten arc operating in high pressure environments", W.J., July 1980, pp. 199s-207s
10. V.A. Malakhovskii, "The influence on arc dimension of plasma torch nozzle design and process variables", Svar. Proiz., 1976, No. 7, pp. 43-45
11. Y. Arata & I. Miyamoto, "Some fundamental properties of high power laser beam as a heat source (report 3)", Trans. of J.W.S., April 1972, pp. 163-170
12. T.W. Eager & S.S. Tsai, "Temperature fields produced by travelling distributed heat sources", W.J., Dec. 1983, pp. 346s-355s
13. D. Rosenthal, "The theory of moving source

of heat and its application to metal treatments", Trans. of A.S.M.E., Nov. 1946, pp.849-864
14. D. Rosenthal, "Methematical theory of heat distribution during welding and cutting", W.J., May 1941, pp.220s-234s
15. I.S. Gradshteyn and I.M. Ryzhik, *Table of integrals, series and products*, Academic press inc., 1980
16. K. Masubuchi, *Analysis of welded structures*, Pergamon press, 1980